ORIGINAL RESEARCH

Kuo et al

Study on the effect of a triple cancer treatment of propolis, thermal cycling-hyperthermia, and low-intensity ultrasound on PANC-1 cells

Yu-Yi Kuo[1,2], Wei-Ting Chen[1,2], Guan-Bo Lin[1,2], Chueh-Hsuan Lu[1,2], and Chih-Yu Chao[1,2,3]

[1] Department of Physics, Lab for Medical Physics & Biomedical Engineering, National Taiwan University, Taipei 10617, Taiwan

[2] Biomedical & Molecular Imaging Center, National Taiwan University College of Medicine, Taipei 10051, Taiwan

[3] Graduate Institute of Applied Physics, Biophysics Division, National Taiwan University, Taipei 10617, Taiwan

Correspondence: Chih-Yu Chao

Department of Physics, Lab for Medical Physics and Biomedical Engineering, National Taiwan University, No 1, Sec 4, Roosevelt Rd, Taipei 10617, Taiwan, Republic of China Tel +886-2-3366-9612

Fax +886-2-3366-5088

E-mail: cychao@phys.ntu.edu.tw (CYC)

Abstract

Background: Pancreatic cancer is a deadly cancer around the world. To reduce side effects and enhance treatment efficacy, study on combination therapy for pancreatic cancer has gained much attention in recent years.

Methods: In this paper, we propose a novel triple treatment combining propolis and two physical stimuli□thermal cycling-hyperthermia (TC-HT) and low-intensity ultrasound (US) on a human pancreatic cancer cell line PANC-1. MTT assay was used to determine the viability of PANC-1 cells. Flow cytometry was used to detect apoptosis, mitochondrial membrane potential (MMP) loss, and intracellular reactive oxygen species (ROS) levels. Western blot analysis was further performed to measure protein expression and phosphorylation.

Results: The experiments found that, after the triple treatment, the cell viability of the PANC-1 cells decreased to a level 80% less than the control, without affecting the normal pancreatic cells. Another result was excessive accumulation of ROS after the triple treatment, leading to the amplification of apoptotic pathway through the mitogen-activated protein kinase (MAPK) family and mitochondrial dysfunction. Moreover, the combination of TC-HT and US also promotes the anticancer effect of the heat-sensitive chemotherapy drug cisplatin on PANC-1 cells.

Conclusion: This study, to the best of our knowledge, is the first attempt to combine TC-HT, US and a nature compound in cancer treatment. We demonstrate that physical stimuli could augment the therapeutical effect of anticancer agents. It is expected that optimized parameters for different agents and different types of cancer will expand the methodology on oncological therapy in a safe manner.

Keywords: combination treatment, synergistic effect, hyperthermia, pancreatic cancer, propolis

Introduction

Cancer is one of the most dreadful diseases and the second leading cause of death around the world. Among all kinds of cancers, pancreatic cancer is the most threatening one, due to its high death rate and low five-year survival rate.[1] Existing therapies for pancreatic cancer, including surgery, radiation, and chemotherapy, all involve major risks, such as tumor recurrence, refractory, and serious side effects,[2] as a result of which development of new therapies is of the utmost importance. A popular option is combination therapy, administering two or more anticancer agents to attain a synergistic effect.[3] However, the interaction between drugs may lead to unexpected competition and even harmful side effects,[4,5] jeopardizing patients' health, let alone improving therapeutic efficacy.

An emerging option in combination therapy is physical stimulus, whose effects on cellular physiology have been reported in several studies.[6-8] Our team has also looked into the feasibility of combing drug therapy and physical stimuli, such as heat,[9] electric field,[10] and magnetic field.[11] Ultrasound (US) is also a therapeutic tool with extensive application, such as developing internal images,[12,13] transporting liposomes to increase agent-delivery rate,[14,15] and ablating tumors from normal tissues.[16,17] The previous study also found US as a helpful method in inhibiting significantly the viability of PANC-1 cells.[18] However, US may also entail a number

of risks, such as harm to normal tissues around tumors due to overheating caused by high-intensity US.[19,20] In addition, liposomes may induce myocardial injury during transport by US.[21,22] In view of this, integrating low-intensity US[23,24] with a non-hazardous agent is important for expanding the use of US in therapy.

Accordingly, the study employed natural compounds from herbal medicines as anticancer agent. Among natural compounds with therapeutic potential, propolis has been found to be effective in inhibiting several cancer cell lines.[25-27] In our previous study, propolis was applied, along with thermal cycling-hyperthermia (TC-HT) as a physical stimulus,[28] in cancer treatment, but the effect still lags behind the in vitro efficacy of chemotherapy drugs.

In this paper, the study introduced low-intensity US as a secondary helper, on top of TC-HT, in order to further augment the anticancer effect of propolis. The novel triple treatment turned out to inhibit the viability of PANC-1 cells significantly, approaching the in vitro efficacy of chemotherapy drugs, without damaging the normal human pancreatic duct cells and skin cells. The study found that the low-intensity US in the triple treatment helped to manipulate the phosphorylation levels of mitogen-activated protein kinase (MAPK) family, thereby activating the intracellular apoptotic signalling. Moreover, it was found in the upstream that

intracellular reactive oxygen species (ROS) also increased greatly after the low-intensity US was applied in the triple treatment, thereby boosting the death rate of PANC-1 cells.

Materials and Methods

Cell culture and propolis treatment

The human pancreatic cancer cell line PANC-1 and the normal human embryonic skin cell line Detroit 551 were obtained from Bioresource Collection and Research Center (Hsinchu, Taiwan). Normal human pancreatic duct H6c7 cells were purchased from Kerafast, Inc. (Boston, MA, USA). PANC-1 and Detroit 551 cells were cultured respectively in DMEM and EMEM (both from Hyclone, South Logan, UT, USA) supplemented with 10% fetal bovine serum (FBS) (Hyclone) and 1% penicillin-streptomycin (Gibco Life Technologies, Grand Island, NY, USA). H6c7 cells were maintained in keratinocyte-serum free medium (Invitrogen, Life Technologies, Grand Island, NY, USA) supplemented with human recombinant epidermal growth factor, bovine pituitary extract (Invitrogen), and 1% penicillin-streptomycin (Gibco Life Technologies). All cells were maintained in a humidified 5% CO_2 incubator at 37 °C and subcultured by 0.05% trypsin–0.5 mM EDTA solution (Gibco Life Technologies). Once the confluences reached

97 suitable percentages, cells were plated in 96-well or 35-mm-diameter culture dishes (Thermo
98 Fisher Scientific, Inc., Waltham, MA, USA) for in vitro experiments after 24 h. Propolis was
99 purchased from Grandhealth™ (Grand Health Inc, Richmond, BC, Canada), and cisplatin was
100 obtained from Sigma-Aldrich (St. Louis, MO, USA). All agents were mixed with culture
101 medium to the desired concentration and were incubated with cells for 1h before treating
102 physical stimuli.
103

104 **Ultrasound exposure**

105 The US exposure system consisted of a function generator (SG382; Stanford Research Systems,
106 Sunnyvale, CA, USA), a power amplifier (25a250a; Amplifier Research, Souderton, PA, USA),
107 and a planar transducer (A104S-RM; Olympus NDT Inc., Waltham, MA, USA). Continuous
108 pulses were produced using the function generator with the following parameters: -10 dBm
109 amplitude, 1 ms pulse period, and 0.5 ms pulse width. The cell culture plate or dish was placed
110 on the ceramic transducer (resonance frequency 2.25 MHz), which converted electrical signals
111 into acoustic power (**Fig 1A**). To avoid undesirable thermal effects induced by US, the output

112 power of the spatial average intensity of the US exposure was adjusted to be 0.3 W/cm^2

113 according to the previous studies.[29,30]

114

115 **Thermal cycling-hyperthermia (TC-HT) treatment**

116 A modified polymerase chain reaction (PCR) system was used to perform TC-HT (Figure 1B).

117 Thermal cycler (model 2720) was purchased from Applied Biosystems (Thermo Fisher

118 Scientific). The system was repeatedly brought to the desired high temperature state and

119 followed by a cooling stage to achieve a series of short period of heat exposure within the

120 desired time (Figure 1C). The experimental setup and administration of TC-HT (10-cycles) have

121 been previously described with optimum results.[28] The actual temperatures the cancer cells

122 sensed were measured by a needle thermocouple, ranging in 45~40.5 °C (Figure 1D).

123 Ultrasound exposure was applied either before or after the TC-HT treatment, for different

124 combination tests. During the TC-HT treatment (~ 45 min), the control and propolis-treated

125 groups were under room temperature (RT) without a 5% CO_2 environment. After the treatments,

126 cells were maintained in the cell culture incubator for the following experiments.

127

128 **MTT assay**

3-(4,5-dimethylthiazol-2-yl)-2,5-diphenyltetrazolium bromide (MTT) (Sigma-Aldrich) was dissolved in distilled water to prepare a 5 mg/ml stock solution. The treated PANC-1 cells were incubated for 4 h at 37 °C with a final MTT concentration 0.5 mg/ml in DMEM culture medium to assess the cell viabilities. The formazan crystals were dissolved by equal volume of the solubilizing buffer of 10% sodium dodecyl sulfate (SDS) (Bioshop Canada Inc., Burlington, ON, Canada) solution in 0.01 N hydrochloric acid (HCl) (Echo Chemical Co. Ltd., Miaoli, Taiwan) at 37 °C overnight. The absorbance of each well was detected by Multiskan GO microplate Spectrophotometer (Thermo Fisher Scientific), and the quantity of formazan was determined by the absorbance at 570 nm, with a background subtraction at 690 nm. The cell viabilities were expressed in percentage and the untreated control was set at 100%.

Treatment with ROS scavenger

PANC-1 cells were seeded into 96-well or 35-mm-diameter culture dishes overnight. For ROS inhibition analysis, cells were pretreated with 5 mM N-acetyl-cysteine (NAC) (Sigma-Aldrich) in culture medium for 1 h and subsequently treated with propolis and/or physical stimuli.

Apoptotic analysis by flow cytometry

PANC-1 cells were collected 24 h after treatments and then rinsed twice with ice-cold phosphate buffered saline (PBS) (Hyclone). The apoptotic rates were analyzed by the Annexin V-FITC and propidium iodide (PI) double detection kit (BD Biosciences, San Jose, CA, USA), and the rinsed cells were resuspended in binding buffer containing Annexin V-FITC and PI and then incubated at RT for 15 min in the dark. Apoptotic signals were detected by FACSCanto II system (BD Biosciences).

ROS and mitochondrial membrane potential (MMP) analyses by flow cytometry

ROS was detected using the fluorescent dye dihydroethidium (DHE) (Sigma-Aldrich), and the loss of MMP was determined using the lipophilic cationic fluorescent dye 3,3'-dihexyloxacarbocyanine iodide ($DiOC_6(3)$) (Enzo Life Sciences, Inc., Plymouth Meeting, PA, USA). PANC-1 cells were harvested 24 h after treatments and rinsed with PBS before staining. Rinsed cells were resuspended and then incubated with 5 μM DHE or 20 nM $DiOC_6(3)$ in PBS at 37 °C for 30 min in the dark. The fluorescence signals were measured by FACSCanto

160 II system (BD Biosciences) with the PE channel (for DHE staining) or FL1 channel (for
161 $DiOC_6(3)$ staining).
162

163 **Western blot analysis**

164 Protein expression levels of PANC-1 cells were quantified by western blot analysis. Cells were
165 rinsed with PBS and then lysed in the lysis buffer (50 mM Tris-HCL, pH 7.4, 0.15 M NaCl,
166 0.25% deoxycholic acid, 1% NP-40, 1% Triton X-100, 0.1 % SDS, 1 mM EDTA) (Millipore,
167 Billerica, MA, USA), supplemented with active protease (Millipore) and phosphatase inhibitor
168 cocktail (Cell signaling Technology, Danvers, MA, USA). After centrifugation, the supernatants
169 were collected and the protein concentrations were quantified by Bradford protein assay
170 (Bioshop, Inc.). Equal amount of proteins (20 μg) were resolved by 10% SDS-polyacrylamide
171 gel electrophoresis (SDS-PAGE) and then transferred onto polyvinylidene fluoride (PVDF)
172 membranes (Millipore). 5% skim milk powder or 5% bovine serum albumin in TBST (20 mM
173 Tris-base, pH 7.6, 0.15 M NaCl, 0.1% Tween 20) was used to block nonspecific antibody
174 binding sites for 1 h at RT. Afterwards, the blocked membranes were probed with specific
175 primary antibodies against phosphorylated extracellular signal-regulated kinases (p-ERK),

phosphorylated c-Jun N-terminal kinase (p-JNK), poly (ADP-ribose) polymerase (PARP) (Cell signaling), phosphorylated p38 MAPK (p-p38), and glyceraldehyde-3-phosphate dehydrogenase (GAPDH) (Gentex, Irvine, CA, USA) at 4 °C overnight. The membranes were rinsed with TBST buffer three times and then incubated with horseradish peroxidase-conjugated goat anti-rabbit secondary antibodies (Jackson ImmunoResearch Laboratories, West Grove, PA, USA) in a blocking solution at RT for 1 h. Immunoreactivity signal was amplified by an enhanced chemiluminescence (ECL) substrate (Advansta, San Jose, CA, USA) and detected by an imaging system Amersham Imager 600 (GE Healthcare Life Sciences). GAPDH was used as the loading control to normalize the relative folds of targeting proteins.

Statistical analysis

Experiments were repeated three times for validation, and statistical analyses were performed using one-way analysis of variance (ANOVA) by OriginPro 2015 software (OriginLab). Results were expressed as the mean ± standard deviation, and were considered to be statistically significant when p-values were less than 0.05.

Results

Triple treatment greatly inhibits the viability of PANC-1 cells

The cell viability of PANC-1 cells versus the propolis concentration was performed in a gradient manner. When the propolis was less than 0.5%, as shown in Figure 2A, there was no notable inhibition effect on MTT results. However, when it exceeded 0.5%, the cell viability dropped significantly. Therefore, a moderate propolis concentration 0.3% was chosen for the following experiments. Next, the physical stimuli of TC-HT and low-intensity US were introduced to affect the viability of PANC-1 cells. In our study, 10-cycles TC-HT and 2.25 MHz US with intensity 0.3W/cm^2 and duration 30 minutes were chosen to avoid the thermotoxicity on PANC-1 cells. As shown in Figure 2B, we found that the combination of TC-HT and US was also innocent to PANC-1 cells, but when 0.3% propolis was involved in the triple treatment, the viability of PANC-1 cells was greatly inhibited. It was also noted that the implementation order of TC-HT and US in triple treatment was influential. When TC-HT was performed prior to US (TC-HT + US) in the presence of 0.3% propolis, US helped to further suppress the cell viability of PANC-1 cells significantly down to 17.1%, cutting more than 80% of the viability of the untreated control and thus approaching the in vitro efficacy of

chemotherapy drugs. In comparison, the treatment that US was performed prior to TC-HT (US + TC-HT) showed a less inhibition effect (43.1% viability), and hence we adopted the implementation order TC-HT + US as the protocol of the triple treatment in the subsequent experiments. Furthermore, in all double treatments, only 0.3% propolis + TC-HT showed notable inhibition effect (48.9% viability) on PANC-1 cells, which was consistent with our previous results.[28] However, 0.3% propolis + US performed a relatively poor inhibition effect (65.4% viability) on PANC-1 cells, and as a result it was also not included in the following experiments. Figure 2C showed the light microscope images of PANC-1 cells 24 h after each treatment, and the cell morphologies demonstrated an evident inhibition effect on PANC-1 cells after the triple treatment. Moreover, normal cells such as the human skin cells Detroit 551 (Figure 2D) and human pancreatic duct cells H6c7 (Figure 2E) were not significantly affected by the triple treatment as well as all the other treatments. The result indicates that the triple treatment could have a good selective effect on carcinoma cells and normal cells, which makes it safer and more feasible in anticancer treatment.

Triple treatment increases intracellular ROS levels synergistically

Intracellular ROS is an important regulator of cell death. It has been reported that heat and low-intensity US could elevate the intracellular ROS level.[31,32] We further investigated whether ROS was increased in response to the triple treatment, so the DHE was used in this experiment to determine the level of superoxide radical anion ($O_2^{\cdot -}$) in PANC-1 cells after each treatment. As shown in Figure 3A-B, it was found that propolis hardly changed the fluorescence signals. Although propolis + TC-HT significantly deformed the fluorescence intensity distribution in an enhanced manner (1.6-fold to control), it did not significantly differ from the enhancement induced by TC-HT alone. In addition, US elevated ROS levels as well, though not as many as TC-HT. Noticeably, the triple treatment showed a significant accumulation of the intracellular ROS (up to 2.1-fold of the control group), which was also significantly higher than the TC-HT + 0.3% propolis treatment. The result suggested that, in the triple treatment, US helped to further boost up the generation of ROS in PANC-1 cells, and could result in enhanced cell death rate after the treatment.

Triple treatment increases mitochondrial apoptosis in PANC-1 cells

It has been known that the enhanced intracellular ROS levels were positively correlated to mitochondrial apoptosis.[33] In our work, the apoptotic rates of PANC-1 cells after various treatments were analyzed by the flow cytometry with the fluorescence dye Annexin V and PI (Figure 4A-B). With the aid of US, the triple treatment further caused 55.3% apoptotic rate, which was significantly higher than the 23.5% apoptotic rate caused by the double treatment of propolis and TC-HT. The cell apoptosis results observed here were highly consistent with the results of the accumulated ROS levels in PANC-1 cells after the same treatment, as described in Figure 3. Furthermore, the mitochondrial membrane potential (MMP) was assessed using $DiOC_6(3)$ fluorescence staining by flow cytometric analysis. As shown in Figure 4C-D, the ratio of the cells exhibiting MMP loss was significantly promoted to 23.3% after the double treatment of propolis + TC-HT, and it was further elevated significantly to 34.7% by employing the triple treatment. These results showed that adopting US in the triple treatment could decrease MMP level, and hence caused more mitochondrial dysfunction. The decreased MMP level was an indicator of mitochondrial apoptosis, and since the results of apoptosis assay (Figure 4A-B) and MMP assay (Figure 4C-D) were quite similar, we believe that the mitochondrial dysfunction was implicated in the apoptosis of PANC-1 cells via the triple treatment.

The apoptosis induced by triple treatment is regulated through MAPK pathway

The activation of apoptotic signalling was examined by western blot analysis. As shown in Figure 5A, we found that the PARP cleavage was significantly increased (2.9-fold of control) after propolis + TC-HT treatment on PANC-1 cells. Noticeably, the PARP cleavage was further promoted significantly to 6.2-fold of control by US in the triple treatment (Figure 5A). Together with the previous flow cytometry results of apoptosis and MMP, it was pointed out that propolis + TC-HT could activate the mitochondrial apoptosis signalling in PANC-1 cells, and US in the triple treatment could further help this cascade to realize a near-chemotherapy level treatment in vitro.

Moreover, it was known that the PARP cleavage could be modulated by MMP level, and mitochondrial dysfunction could also be regulated by the excessive intracellular ROS via MAPK family.[34] In MAPK family, the p-ERK level represented the activation of cell survival,[35] while the p-JNK and p-p38 levels were the indicator of cell death.[36,37] In this study, it was found that the p-ERK level was suppressed by propolis + TC-HT treatment (0.30-fold), and was further down-regulated when US was introduced in the triple treatment (0.15-fold) (Figure 5B).

In addition, the p-JNK and p-p38 levels both exhibited a reverse performance, which were promoted the most in the triple treatment (8.7-fold & 9.2-fold, respectively) (Figure 5C-D). These results were consistent with the results of ROS and MMP assessments by flow cytometry. Therefore, we speculated that the excess intracellular ROS induced by the triple treatment regulated the activation of the MAPK family and thus caused mitochondrial dysfunction and the cascade of apoptosis.

ROS scavenger attenuates the apoptosis induced by triple treatment

To further confirm that the cell death after the triple treatment was regulated by the generation of intracellular ROS, the ROS scavenger NAC was applied in the experiment.[38] 5 mM NAC was incubated with PANC-1 cells 1 h prior to the triple treatment. As shown in Figure 6A, the inhibitory effect of the triple treatment was restored by NAC, and NAC itself did not affect the viability of PANC-1 cells. Similar results were also observed in the activation of apoptotic pathway, as shown in Figure 6B. NAC alone did not affect PARP cleavage, but it significantly down-regulated the triple treatment-promoted PARP cleavage (Figure 6B). Therefore, the

287 results supported our speculation that the triple treatment could induce mitochondrial apoptosis
288 of PANC-1 cells via the excessive increment of intracellular ROS.
289

290 **Triple treatment can be applied with chemotherapy drug as a novel anticancer**
291 **treatment**

292 In this study, we have shown that the method TC-HT followed by mild US exposure could
293 further amplify the anticancer effect of propolis. But, the question is whether the TC-HT + US
294 method can be expanded to the existing chemotherapy drugs. Cisplatin, for instance, was a
295 commonly used clinical chemotherapy drug for several kinds of cancers such as lung, ovarian,
296 breast, and brain cancer.[39] Besides, it has also been reported that cisplatin was sensitive to
297 heat.[40] However, the conventional therapeutic dosage of cisplatin could cause severe side effects
298 to the patients,[41,42] and therefore it was important to develop a new method to reduce the
299 effective dose of cisplatin. As a result, we applied the method of TC-HT + US with cisplatin on
300 the PANC-1 cells to investigate the potential of this triple treatment method. A relatively low
301 dose of 1 μM cisplatin and short incubation time 24 h was chosen for the MTT assay
302 independently or in combination with the physical stimulations. [43,44] After the treatment, the

viability of PANC-1 cells was just slightly inhibited by 7.5% by individual cisplatin, and the double treatment of cisplatin + TC-HT also did not alter the viability of PANC-1 cells. The triple treatment, however, promoted the inhibitory effect significantly up to 48.2% (Figure 7). Compared to the conventional results of cisplatin, our method could not only reduce the effective dose but also boost up the anticancer effect of cisplatin. Therefore, the method of physical stimuli in the study should hold great potential to apply onto other heat sensitive chemotherapy drugs or anticancer agents to achieve a better anticancer effect.

Discussion

Combination treatment augments the anticancer effect of individual agents by activating multiple pathways, thereby lowering the necessary dosage of the agents to a level harmless to normal cells and human health. However, research on combination anticancer agents is costly and time-consuming.[45] Moreover, unpredictable molecular interactions may be detrimental to patients' health.[5] Therefore, the application of physical stimuli has been considered as a potential candidate for combinative anticancer treatments in combating cancer. Following several combination treatments of physical stimuli and herbal compounds proposed by our team previously,[46] the study put forth the combination treatment of propolis, TC-HT, and

low-intensity US, proving that it can inhibit pancreatic cancer cell line PANC-1 at a level close to the in vitro efficacy of chemotherapy drugs.

In cancer cells, intracellular ROS levels have been known to be the main source of the oxidative stress,[47] a key factor for cell viability.[48] Elevated ROS level has been shown to be able to activate some signalling pathways associated with cell proliferation, apoptosis, and cell cycle progression.[49] Besides, heat treatment and low-intensity US both can increase the intracellular ROS levels.[31,32] In this work, the study shows that TC-HT significantly augments the intracellular ROS levels of PANC-1 cells (Figure 3A-B), at an extent higher than the individual effects of propolis and low-intensity US. It was found that the combination of propolis and TC-HT did not further elevate the levels in PANC-1 cells. Nevertheless, after the low-intensity US was administered, the triple treatment showed a great improvement effect, doubling the intracellular ROS levels of PANC-1 cells. It has been known that excessive intracellular ROS level could activate the apoptotic pathway cascade, increasing the apoptosis in the carcinoma cells.[33] Our study demonstrated that the apoptotic rate of PANC-1 cells was elevated along with the increase of the intracellular ROS levels. The result showed that the triple treatment induced the highest apoptotic rate, compared with other approaches, suggesting its ability to regulate the death of PANC-1 cells via excessive intracellular ROS accumulation. To demonstrate the

crucial role of the intracellular ROS levels, NAC was employed in the following experiments on the triple treatment. While independent NAC pretreatment did not affect the viabilities of PANC-1 cells (Figure 6A), it protected the cells from cytotoxicity in the triple treatment. Hence, ROS elevation played a key role in the anticancer effect in the triple treatment.

The initiation of apoptosis, a common cell death mechanism, is closely related to the function of mitochondria, which is the chemical-energy source of cells and critical for the viability of cells.[50] It was reported that US could induce mitochondrial dysfunction,[51] and the dysfunction could induce a series of biochemical cascade of apoptosis, thereby blocking cell proliferation.[52] Meanwhile, the activated members of the MAPK family, such as ERK, JNK, and p38 were deemed to be capable of regulating the dysfunction of mitochondria, and the elevated ROS level was shown to be conducive to the activation of p38 and JNK but down-regulate the activation of ERK.[53] The results suggest that excessive ROS further induced by US could cause greater mitochondrial apoptotic rate via additionally activating the MAPK family members. In this work, our study showed that adopting US in the triple treatment raised greater apoptotic rate of PANC-1 cells (Figure 4A-B), while decreasing the MMP level lower, which led to more severe dysfunction of mitochondria than the double treatment of propolis and TC-HT (Figure 4C-D). Furthermore, the mild US in the triple treatment further helped to increase the

354 phosphorylated levels of p38 and JNK significantly, while inhibiting the phosphorylation of
355 ERK (Figure 5), underscoring its ability to manipulate the function of mitochondria via the
356 ROS-activated MAPK family proteins.

357 The injured mitochondria would release cytochrome-c into the cytoplasm,[54] cleaving
358 caspase 9 and thus activating caspase 3 in the downstream,[55] which entered further the nucleus
359 and cleaved PARP. Then PARP would lose its enzyme activity, initiating apoptosis
360 irreversibly.[56] In addition, it was reported that US could induce mitochondrial apoptosis in
361 cancer cells.[51,57] The study demonstrated that the triple treatment could induce mitochondrial
362 dysfunction via regulating the phosphorylation level of the members of MAPK family. In
363 addition, the triple treatment also increased PARP cleavage significantly, compared with the
364 combination treatment of propolis and TC-HT (Figure 5A). Furthermore, as shown in Figure 6B,
365 it was found that the triple treatment-promoted PARP cleavage was significantly suppressed by
366 NAC, which indicates that increased ROS level was the key regulator for the apoptotic effect of
367 the triple treatment.

368 The triple treatment in the study included two physical stimuli, TC-HT and US, which
369 could be integrated for simultaneous implementation via the high-intensity focused ultrasound
370 (HIFU). Being able to raise temperature in the exposed region for energy transfer,[19,20] HIFU has

been applied for tumor ablation for over a decade.[16,58] The temperature increase could be electrically controlled and directed to the targeted region.[59] Therefore, with the help of HIFU, the triple treatment could be applied clinically. To augment the effect, cisplatin, a common thermal sensitive chemotherapy drug, was incorporated as a substitute for propolis into the triple treatment. It was shown that the inhibited viability of PANC-1 cells by cisplatin was further suppressed with a large extent when both of TC-HT and US were introduced into the treatment (Figure 7). The dosage of cisplatin can be reduced to a lower concentration, without compromising the anticancer effect. As a result, the triple treatment has the potential supplementing the administration of drugs, not only augmenting the effect but also reducing the dosage of the latter.

Conclusion

In summary, this study proposed for the first time an effective triple cancer treatment combining propolis, TC-HT, and low-intensity US, which could significantly suppress the growth of PANC-1 cells via an ROS-modulated mitochondrial apoptosis, with a performance comparable to chemotherapy. The study also showed that the triple treatment could induce mitochondrial dysfunction via the regulation of MAPK family, resulting in apoptosis via the

388 up-regulated PARP cleavage. It also demonstrated that the ROS level plays a key role in the
389 performance of the triple treatment. In addition, chemotherapy drugs, such as cisplatin, can be
390 incorporated into the treatment as substitute for propolis. The triple treatment incorporating
391 cisplatin also exhibited a much higher effect in inhibiting cancer cell growth than the cisplatin
392 alone, promising to increase the performance and safety of the existing cancer therapy. Overall,
393 the study proposed employment of physical stimuli, as a promising option in cancer therapy.
394

395 Acknowledgments

396 The authors would like to acknowledge the service provided by Technology
397 Commons in College of Life Science, National Taiwan University for use of flow
398 cytometry system. This work was supported by grants from Ministry of Science and
399 Technology (MOST 110-2112-M-002-004, MOST 109-2112-M-002-004, and MOST
400 108-2112-M-002-016 to CYC) and Ministry of Education (MOE 106R880708 to CYC)
401 of the Republic of China. The funders had no role in study design, data collection and
402 analysis, decision to publish, or preparation of the manuscript.
403

404 Disclosure

405 The authors have declared that no competing interests exist.

406

407 # References

408 1. Siegel RL, Miller KD, Jemal A. Cancer statistics, 2019. *CA Cancer J Clin*. 2019;69(1):
409 7-34.

410 2. Lee JC, Ahn S, Cho IK, Lee J, Kim J, Hwang JH. Management of recurrent pancreatic
411 cancer after surgical resection: a protocol for systematic review, evidence mapping and
412 meta-analysis. *BMJ Open*. 2018;8(4):e017249.

413 3. Yap TA, Omlin A, de Bono JS. Development of therapeutic combinations targeting
414 major cancer signaling pathways. *J Clin Oncol*. 2013;31(12):1592-1605.

415 4. Terrault NA. Benefits and risks of combination therapy for hepatitis B. *Hepatology*.
416 2009;49 (5 Suppl):S122-S128.

417 5. Lee JJ, Kong M, Ayers GD, Lotan R. Interaction index and different methods for
418 determining drug interaction in combination therapy. *J Biopharm Stat*.
419 2007;17(3):461-480.

6. Soares PI, Ferreira IM, Igreja RA, Novo CM, Borges JP. Application of hyperthermia for cancer treatment: recent patents review. *Recent Pat Anticancer Drug Discov*. 2012;7(1):64-73.

7. Davies AM, Weinberg U, Palti Y. Tumor treating fields: a new frontier in cancer therapy. *Ann N Y Acad Sci*. 2013;1291(1):86-95.

8. Wood AKW, Sehgal CM. A review of low-intensity ultrasound for cancer therapy. *Ultrasound Med Biol*. 2015;41(4):905-928.

9. Lu CH, Chen WT, Hsieh CH, Kuo YY, Chao CY. Thermal cycling-hyperthermia in combination with polyphenols, epigallocatechin gallate and chlorogenic acid, exerts synergistic anticancer effect against human pancreatic cancer PANC-1 cells. *PLoS One*. 2019;14(5):e0217676.

10. Lu CH, Lin SH, Hsieh CH, Chen WT, Chao CY. Enhanced anticancer effects of low-dose curcumin with non-invasive pulsed electric field on PANC-1 cells. *Onco Targets Ther*. 2018;11:4723-4732.

11. Chen WT, Lin GB, Lin SH, et al. Static magnetic field enhances the anticancer efficacy of capsaicin on HepG2 cells via capsaicin receptor TRPV1. *PLoS One*. 2018;13(1):e0191078.

12. O'Keeffe D, Mamtora H. Ultrasound in clinical orthopaedics. *J Bone Joint Surg*. 1992;74(4):488-494.

13. Bendick PJ, Brown OW, Hernandez D, Glover JL, Bove PG. Three-dimensional vascular imaging using Doppler ultrasound. *Am J Surg*. 1998;176(2):183-187.

14. Ferrara K, Pollard R, Borden M. Ultrasound microbubble contrast agents: fundamentals and application to gene and drug delivery. *Annu Rev Biomed Eng*. 2007;9(1):415-447.

15. Wang TY, Wilson KE, Machtaler S, Willmann JK. Ultrasound and microbubble guided drug delivery: mechanistic understanding and clinical implications. *Curr Pharm Biotechnol*. 2013;14(8):743-752.

16. Zhou YF. High intensity focused ultrasound in clinical tumor ablation. *World J Clin Oncol*. 2011;2(1):8-27.

17. Lang BH, Wu ALH. High intensity focused ultrasound (HIFU) ablation of benign thyroid nodules – a systematic review. *J Ther Ultrasound*. 2017;5(1):11.

18. Hsieh CH, Lu CH, Kuo YY, Chen WT, Chao CY. Studies on the non-invasive anticancer remedy of the triple combination of epigallocatechin gallate, pulsed electric field, and ultrasound. *PLoS One*. 2018;13(8):e0201920.

19. van den Bijgaart RJ, Eikelenboom DC, Hoogenboom M, Fütterer JJ, den Brok MH, Adema GJ. Thermal and mechanical high-intensity focused ultrasound: perspectives on tumor ablation, immune effects and combination strategies. *Cancer Immunol Immunother*. 2017;66(2):247-258.

20. Dubinsky TJ, Cuevas C, Dighe MK, Kolokythas O, Hwang JH. High-intensity focused ultrasound: current potential and oncologic applications. *AJR Am J Roentgenol.* 2008;190(1):191-199.

21. Zhang B, Zhou H, Cheng Q, Lei L, Hu B. Low-frequency low energy ultrasound combined with microbubbles induces distinct apoptosis of A7r5 cells. *Mol Med Rep*. 2014;10(6):3282-3288.

22. Vancraeynest D, Havaux X, Pasquet A, et al. Myocardial injury induced by ultrasound-targeted microbubble destruction: evidence for the contribution of myocardial ischemia. *Ultrasound Med Biol*. 2009;35(4):672-679.

23. Johns LD. Nonthermal effects of therapeutic ultrasound: the frequency resonance hypothesis. *J Athl Train.* 2002;37(3):293-299.

24. Bazou D, Maimon N, Munn LL, Gonzalez I. Effects of low intensity continuous ultrasound (LICU) on mouse pancreatic tumor explants. *Appl Sci*. 2017;7(12):1275.

25. Taira N, Nguyen BC, Be Tu PT, Tawata S. Effect of Okinawa propolis on PAK1 activity, caenorhabditis elegans longevity, melanogenesis, and growth of cancer cells. *J Agric Food Chem.* 2016;64(27):5484-5489.

26. Li H, Kapur A, Yang JX, et al. Antiproliferation of human prostate cancer cells by ethanolic extracts of Brazilian propolis and its botanical origin. *Int J Oncol.* 2007;31(3):601-606.

27. Xuan H, Li Zhen, Yan H, et al. Antitumor activity of Chinese propolis in human breast cancer MCF-7 and MDA-MB-231 cells. *Evid Based Complement Alternat Med.* 2014;2014:280120.

28. Chen WT, Sun YK, Lu CH, Chao CY. Thermal cycling as a novel thermal therapy to synergistically enhance the anticancer effect of propolis on PANC□1 cells. *Int J Oncol.* 2019;55(3):617-628.

29. Love L, Kremkau F. Intracellular temperature distribution produced by ultrasound. *J Acoust Soc Am*.1980;67(3):1045-1050.

30. Nahirnyak V, Mast TD, Holland CK. Ultrasound-induced thermal elevation in clotted blood and cranial bone. *Ultrasound Med Biol*. 2007;33(8):1285-1295.

31. Hou CH, Lin FL, Hou SM, Liu JF. Hyperthermia induces apoptosis through endoplasmic reticulum and reactive oxygen species in human osteosarcoma cells. *Int J Mol Sci*. 2014;15(10):17380-17395.

32. Xia C, Zeng H, Zheng Y. Low-intensity ultrasound enhances the antitumor effects of doxorubicin on hepatocellular carcinoma cells through the ROS-miR-21-PTEN axis. *Mol Med Rep*. 2020;21(3):989-998.

33. Redza-Dutordoir M, Averill-Bates DA. Activation of apoptosis signalling pathways by reactive oxygen species. *Biochim Biophys Acta*. 2016;1863(12):2977-2992.

34. Zang YQ, Feng YY, Luo YH, et al. Quinalizarin induces ROS-mediated apoptosis via the MAPK, STAT3 and NF-κB signaling pathways in human breast cancer cells. *Mol Med Rep*. 2019;20(5):4576-4586.

35. Meng J, Fang B, Liao Y, Chresta CM, Smith PD, Roth JA. Apoptosis induction by MEK inhibition in human lung cancer cells is mediated by Bim. *PLoS One*. 2010;5(9):e13026.

36. Chiyo T, Fujita K, Iwama H, et al. Galectin-9 induces mitochondria-mediated apoptosis of esophageal cancer in vitro and in vivo in a xenograft mouse model. *Int J Mol Sci*. 2019;20(11):2634.

503 37. Wu YJ, Su TR, Dai GF, Su JH, Liu CI. Flaccidoxide-13-acetate-induced apoptosis in
504 human bladder cancer cells is through activation of p38/JNK, mitochondrial
505 dysfunction, and endoplasmic reticulum stress regulated pathway. *Mar Drugs*.
506 2019;17(5):287.
507 38. Aruoma OI, Halliwell B, Hoey BM, Butler J. The antioxidant action of
508 N-acetylcysteine: its reaction with hydrogen peroxide, hydroxyl radical, superoxide,
509 and hypochlorous acid. *Free Radic Biol Med*. 1989;6(6):593-597.
510 39. Dasari S, Tchounwou PB. Cisplatin in cancer therapy: molecular mechanisms of action.
511 *Eur J Pharmacol*. 2014;740:364-378.
512 40. Behrouzkia Z, Joveini Z, Keshavarzi B, Eyvazzadeh N, Aghdam RZ. Hyperthermia:
513 how can it be used? *Oman Med J*. 2016;31(2):89-97.
514 41. Florea AM, Büsselberg D. Cisplatin as an anti-tumor drug: cellular mechanisms of
515 activity, drug resistance and induced side effects. *Cancers*. 2011;3(1):1351-1371.
516 42. Ghosh S. Cisplatin: the first metal based anticancer drug. *Bioorg Chem*.
517 2019;88:102925.

518 43. Cregan IL, Dharmarajan AM, Fox SA. Mechanisms of cisplatin-induced cell death in
519 malignant mesothelioma cells: Role of inhibitor of apoptosis proteins (IAPs) and
520 caspases. *Int J Oncol*. 2013;42(2):444-452.
521 44. Beer M, Kuppalu N, Stefanini M, et al. A novel microfluidic 3D platform for culturing
522 pancreatic ductal adenocarcinoma cells: comparison with in vitro cultures and in vivo
523 xenografts. *Sci Rep*. 2017;7(1):1325.
524 45. Huang H, Zhang P, Qu XA, Sanseau P, Yang L. Systematic prediction of drug
525 combinations based on clinical side-effects. *Sci Rep*. 2014;4(1):7160.
526 46. Lu CH, Kuo YY, Lin GB, Chen WT, Chao CY. Application of non-invasive
527 low-intensity pulsed electric field with thermal cycling-hyperthermia for synergistically
528 enhanced anticancer effect of chlorogenic acid on PANC-1 cells. *PLoS ONE*.
529 2020;15(1):e0222126.
530 47. Liou GY, Storz P. Reactive oxygen species in cancer. *Free Radic Res*.
531 2010;44(5):479-496.
532 48. Kannan K, Jain SK. Oxidative stress and apoptosis. *Pathophysiology*.
533 2000;7(3):153-163.

534 49. Aggarwal V, Tuli HS, Varol A, Thakral F, Yerer MB, Sak K. Role of reactive oxygen
535 species in cancer progression: molecular mechanisms and recent advancements.
536 *Biomolecules*. 2019;9(11):735.
537 50. Osellame LD, Blacker TS, Duchen MR. Cellular and molecular mechanisms of
538 mitochondrial function. *Best Pract Res Clin Endocrinol Metab*. 2012;26(6):711-723.
539 51. Wang P, Leung AW, Xu C. Low-intensity ultrasound-induced cellular destruction and
540 autophagy of nasopharyngeal carcinoma cells. *Exp Ther Med*. 2011;2(5):849-852.
541 52. Elmore S. Apoptosis: a review of programmed cell death. *Toxicol Pathol*.
542 2007;35(4):495-516.
543 53. Yuan L, Wang J, Xiao H, Wu W, Wang Y, Liu X. MAPK signaling pathways regulate
544 mitochondrial-mediated apoptosis induced by isoorientin in human hepatoblastoma
545 cancer cells. *Food Chem Toxicol*. 2013;53:62-68.
546 54. Garrido C, Galluzzi L, Brunet M, Puig PE, Didelot C, Kroemer G. Mechanisms of
547 cytochrome c release from mitochondria. *Cell Death Differ*. 2006;13(9):1423-1433.
548 55. Brentnall M, Rodriguez-Menocal L, De Guevara RL, Cepero E, Boise LH. Caspase-9,
549 caspase-3 and caspase-7 have distinct roles during intrinsic apoptosis. *BMC Cell Biol*.
550 2013;14(1):32.

551 56. Jimenez F, Aiba□Masago S, Al Hashimi I, et al. Activated caspase 3 and cleaved
552 poly(ADP-ribose)polymerase in salivary epithelium suggest a pathogenetic mechanism
553 for Sjögren's syndrome. *Rheumatology*. 2002;41(3):338-342.
554 57. Feng Y, Tian Z, Wan M. Bioeffects of low-intensity ultrasound in vitro: apoptosis,
555 protein profile alteration, and potential molecular mechanism. *J Ultrasound Med*.
556 2010;29(6):963-974.
557 58. Duc NM, Keserci B. Emerging clinical applications of high-intensity focused
558 ultrasound. *Diagn Interv Radiol*. 2019;25(5):398-409.
559 59. Park S, Pham NT, Huynh HT, Kang HW. Development of temperature
560 controller-integrated portable HIFU driver for thermal coagulation. *Biomed Eng Online*.
561 2019;18(1):77.

562

563 **Figure 1** Experimental setups for the triple treatment.

564 **Notes:** 35-mm culture dishes were placed on (**A**) a ceramic transducer and (**B**) a modified PCR
565 machine for the exposures of US and TC-HT, respectively. (**C**) The schematic representation of
566 the TC-HT temperature settings. (**D**) Cell temperature detected by a needle thermocouple when

567 TC-HT was implemented. (**E**) Experimental schedule of the triple treatment with different

568 exposing order of US and TC-HT.

569 **Abbreviations:** US, ultrasound; TC-HT, thermal cycling-hyperthermia.

570

571 **Figure 2** Viability inhibition effects of propolis on PANC-1, Detroit 551, and H6c7 cells.

572 **Notes:** MTT assay was conducted to determine the viabilities of PANC-1 cells after the

573 treatment of (**A**) different propolis concentrations and (**B**) different combinations of physical

574 stimulations. (**C**) Representative light microscope images of PANC-1 cells after each treatment,

575 scale bar = 100 μm. The viabilities of (**D**) normal human skin cells Detroit 551 and (**E**) normal

576 human pancreatic duct cells H6c7 were measured 24 h after each treatment. Data were

577 presented as the mean ± standard deviation in triplicate (***P<0.001). Ctrl, Control group with

578 no treatment; Propolis, Propolis group with 0.3% (v/v) propolis; TC-HT, TC-HT group with 10

579 cycles TC-HT (setting: 46 °C 3 min – 37 °C 30 s); Propolis + TC-HT, Propolis + TC-HT group

580 with 0.3% (v/v) propolis and 10 cycles TC-HT (setting: 46 °C 3 min – 37 °C 30 s), sequentially;

581 US, US group with 2.25 MHz US (0.3 W/cm^2) for 30 min; Triple, Triple group with 0.3% (v/v)

582 propolis, 10 cycles TC-HT (setting: 46 °C 3 min – 37 °C 30 s), and 2.25 MHz US (0.3 W/cm^2)

583 for 30 min, sequentially.

584 **Abbreviations:** US, ultrasound; TC-HT, thermal cycling-hyperthermia.

585

586 **Figure 3** The triple treatment raised the generation of intracellular ROS.

587 **Notes:** (**A**) Intracellular superoxide radical anion ($O_2^{\cdot -}$) levels of PANC-1 cells were

588 determined by flow cytometry with the fluorescent dye DHE. (**B**) Quantification of the mean

589 DHE fluorescence levels after each treatment. Data were presented as the mean ± standard

590 deviation in triplicate (***P<0.001). Ctrl, Control group with no treatment; Propolis, Propolis

591 group with 0.3% (v/v) propolis; TC-HT, TC-HT group with 10 cycles TC-HT (setting: 46 °C 3

592 min – 37 °C 30 s); Propolis + TC-HT, Propolis + TC-HT group with 0.3% (v/v) propolis and 10

593 cycles TC-HT (setting: 46 °C 3 min – 37 °C 30 s), sequentially; US, US group with 2.25 MHz

594 US (0.3 W/cm^2) for 30 min; Triple, Triple group with 0.3% (v/v) propolis, 10 cycles TC-HT

595 (setting: 46 °C 3 min – 37 °C 30 s), and 2.25 MHz US (0.3 W/cm^2) for 30 min, sequentially.

596 **Abbreviations:** US, ultrasound; TC-HT, thermal cycling-hyperthermia; DHE, dihydroethidium.

597

598 **Figure 4** Triple treatment increased apoptosis on PANC-1 cells via mitochondrial dysfunction.

599 **Notes:** (**A**) Apoptosis after treatment was analyzed via flow cytometry with Annexin V-FITC/PI

600 double staining, and (**B**) the apoptotic percentage (Q2+Q4) were calculated. (**C**) MMP level

after treatment was analyzed via flow cytometry with $DiOC_6(3)$ staining, and (**D**) the percentage of cells with the loss of MMP (M1) was calculated. Data were presented as the mean ± standard deviation in triplicate (***P<0.001, **P<0.01). Ctrl, Control group with no treatment; Propolis, Propolis group with 0.3% (v/v) propolis; TC-HT, TC-HT group with 10 cycles TC-HT (setting: 46 °C 3 min – 37 °C 30 s); Propolis + TC-HT, Propolis + TC-HT group with 0.3% (v/v) propolis and 10 cycles TC-HT (setting: 46 °C 3 min – 37 °C 30 s), sequentially; US, US group with 2.25 MHz US (0.3 W/cm^2) for 30 min; Triple, Triple group with 0.3% (v/v) propolis, 10 cycles TC-HT (setting: 46 °C 3 min – 37 °C 30 s), and 2.25 MHz US (0.3 W/cm^2) for 30 min, sequentially.

Abbreviations: US, ultrasound; TC-HT, thermal cycling-hyperthermia; $DiOC_6(3)$, 3,3'-dihexyloxacarbocyanine iodide.

Figure 5 Triple treatment modulated apoptosis via regulating the MAPK family.

Notes: Representative western blots of the apoptosis-related proteins and the quantification of (**A**) the PARP cleavage (ratio of cleaved PARP/full length PARP), the phosphorylation level of (**B**) ERK, (**C**) JNK, and (**D**) p38. GAPDH was used as loading control. Data were presented as the mean ± standard deviation in triplicate (***P<0.001, **P<0.01, *P<0.05). Ctrl, Control

group with no treatment; Propolis, Propolis group with 0.3% (v/v) propolis; TC-HT, TC-HT group with 10 cycles TC-HT (setting: 46 °C 3 min – 37 °C 30 s); Propolis + TC-HT, Propolis + TC-HT group with 0.3% (v/v) propolis and 10 cycles TC-HT (setting: 46 °C 3 min – 37 °C 30 s), sequentially; US, US group with 2.25 MHz US (0.3 W/cm^2) for 30 min; Triple, Triple group with 0.3% (v/v) propolis, 10 cycles TC-HT (setting: 46 °C 3 min – 37 °C 30 s), and 2.25 MHz US (0.3 W/cm^2) for 30 min, sequentially.

Abbreviations: US, ultrasound; TC-HT, thermal cycling-hyperthermia.

Figure 6 ROS inhibition blocked the cell death and the activation of apoptosis pathways.

Notes: (**A**) Cell viabilities of PANC-1 cells and (**B**) the quantification of PARP cleavage (ratio of cleaved PARP/full length PARP) after the triple treatment with or without 1h NAC pretreatment. GAPDH was used as loading control. Data were presented as the mean ± standard deviation in triplicate (***P<0.001, **P<0.01). Ctrl, Control group with no treatment; Triple, Triple group with 0.3% (v/v) propolis, 10 cycles TC-HT (setting: 46 °C 3 min – 37 °C 30 s), and 2.25 MHz US (0.3 W/cm^2) for 30 min, sequentially. NAC, NAC group with 5 mM NAC; NAC + Triple, NAC + Triple group with 5 mM NAC prior to the triple treatment.

Abbreviation: NAC, N-acetyl-cysteine.

Figure 7 The method of triple treatment promoted the inhibitory effect of the heat sensitive chemotherapy drug cisplatin.

Notes: Cell viabilities of PANC-1 cells treated with cisplatin, cisplatin + TC-HT, and the triple treatment of cisplatin + TC-HT + US. Cisplatin concentrations in all treatments were 1 μM. Data were presented as the mean ± standard deviation in triplicate (***P<0.001). Ctrl, Control group with no treatment; Cisplatin, Cisplatin group with 1 μM cisplatin; Cisplatin + TC-HT, Cisplatin + TC-HT group with 1 μM cisplatin, 10 cycles TC-HT (setting: 46 °C 3 min – 37 °C 30 s), sequentially; Triple, Triple group with 1 μM cisplatin, 10 cycles TC-HT (setting: 46 °C 3 min – 37 °C 30 s), and 2.25 MHz US (0.3 W/cm^2) for 30 min, sequentially.

Abbreviation: TC-HT, thermal cycling-hyperthermia.

Figure 1

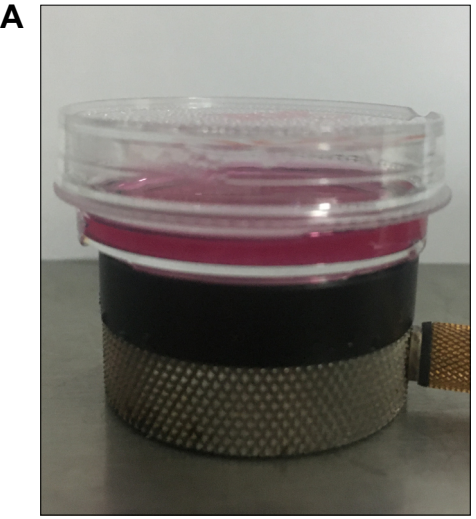
A

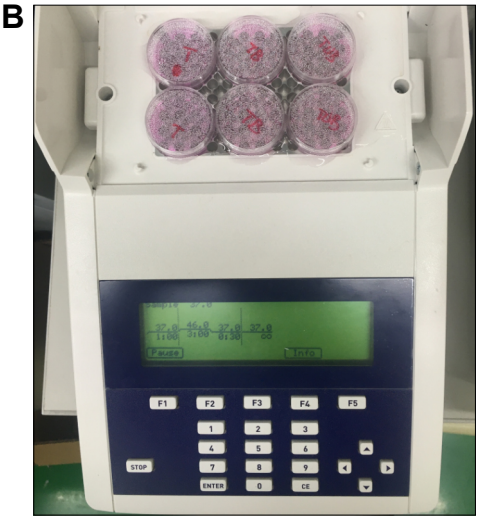
B

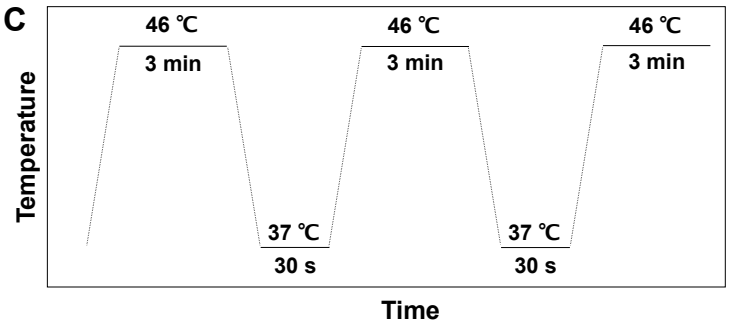
C
46 ℃
3 min
37 ℃
30 s
46 ℃
3 min
37 ℃
30 s
46 ℃
3 min
Temperature
Time

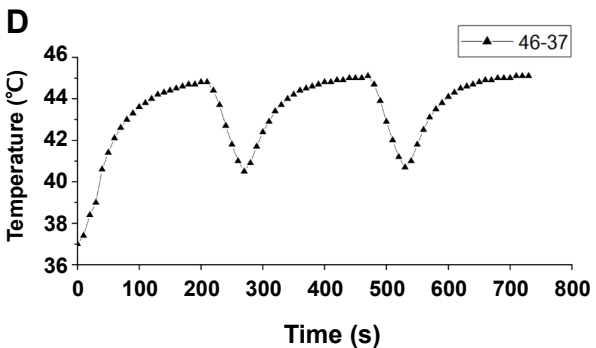
D
46-37
Temperature (℃)
46
44
42
40
38
36
0
100
200
300
400
500
600
700
800
Time (s)

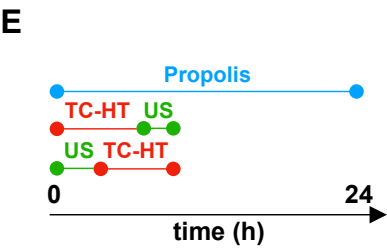
E
Propolis
TC-HT
US
US
TC-HT
0
24
time (h)

Figure 2

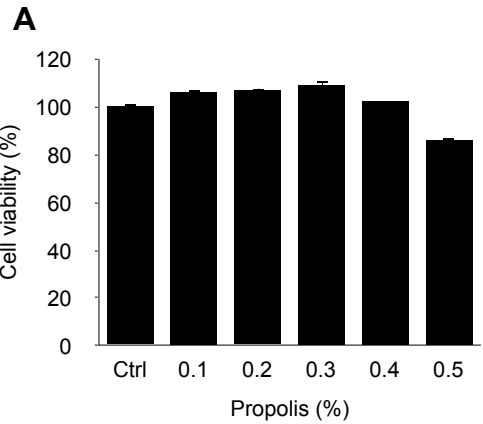
A
120
100
80
60
40
20
0
Cell viability (%)
Ctrl
0.1
0.2
0.3
0.4
0.5
Propolis (%)

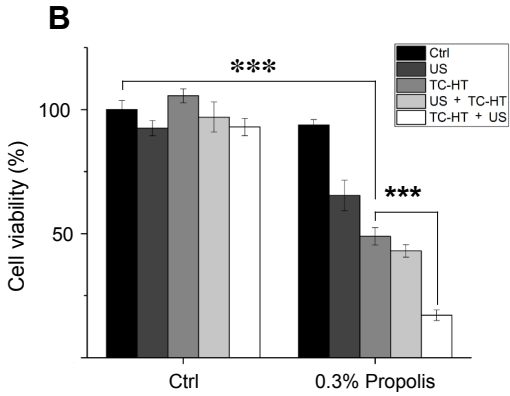
B
***
***
100
50
Cell viability (%)
Ctrl
US
TC-HT
US + TC-HT
TC-HT + US
Ctrl
0.3% Propolis

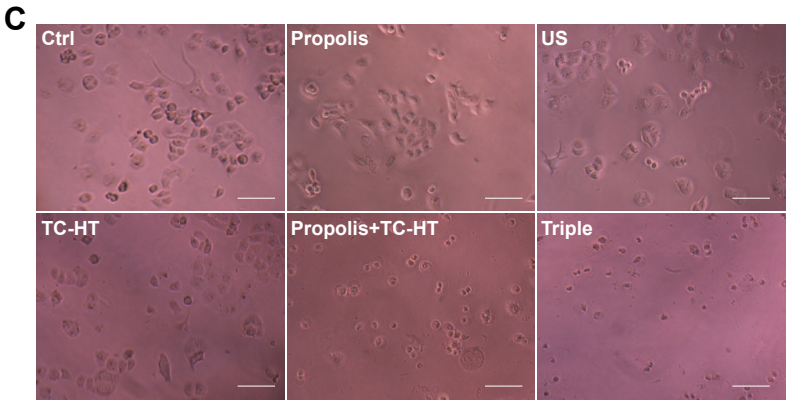
C
Ctrl
Propolis
US
TC-HT
Propolis+TC-HT
Triple

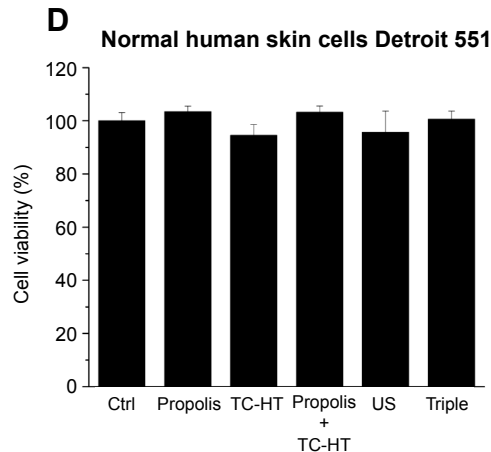
D
Normal human skin cells Detroit 551
120
100
80
60
40
20
0
Cell viability (%)
Ctrl
Propolis
TC-HT
Propolis + TC-HT
US
Triple

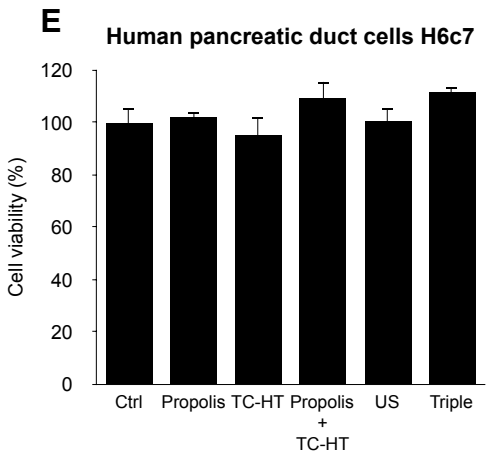
E
Human pancreatic duct cells H6c7
120
100
80
60
40
20
0
Cell viability (%)
Ctrl
Propolis
TC-HT
Propolis + TC-HT
US
Triple

Figure 3

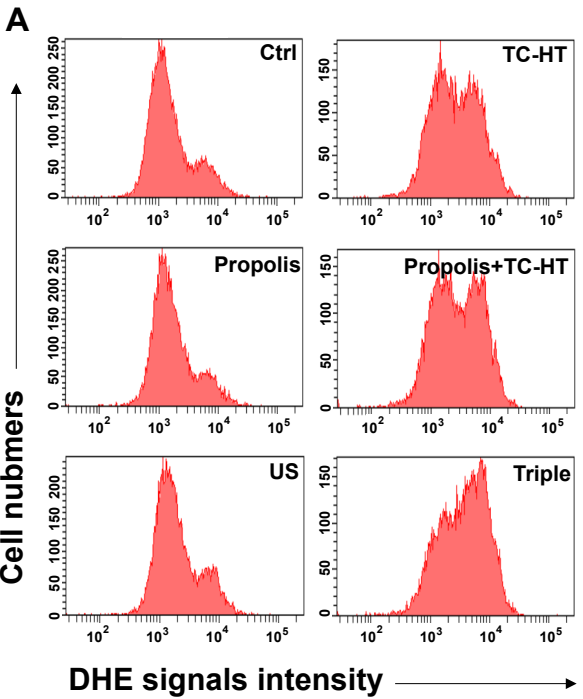
A
Ctrl
TC-HT
Propolis
Propolis+TC-HT
US
Triple
Cell nubmers
DHE signals intensity

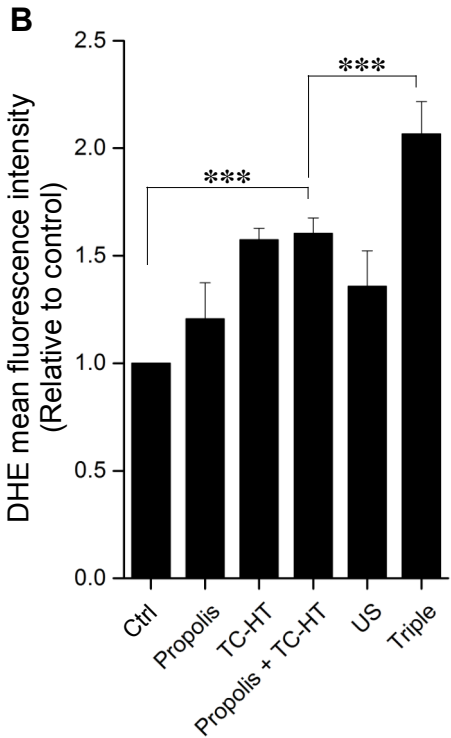
B
DHE mean fluorescence intensity
(Relative to control)
***
***
Ctrl
Propolis
TC-HT
Propolis + TC-HT
US
Triple

Figure 4

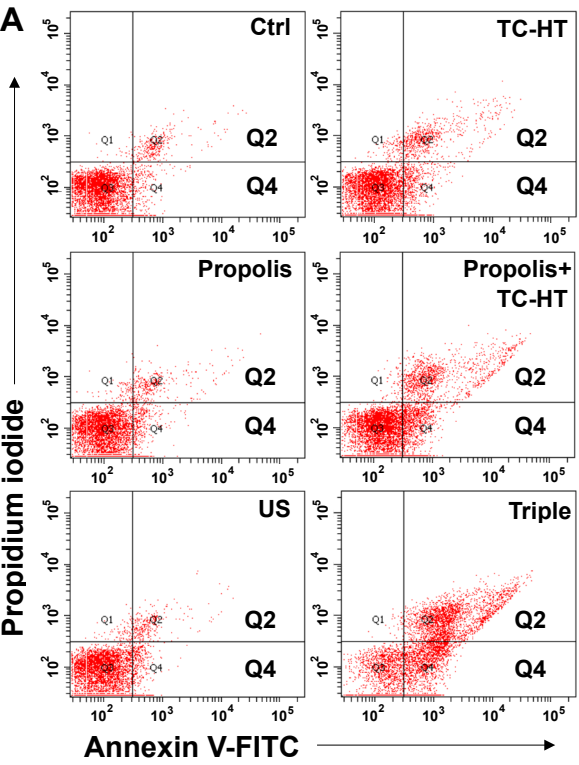
A
Ctrl
TC-HT
Propolis
Propolis+
TC-HT
US
Triple
Q1
Q2
Q3
Q4
Propidium iodide
Annexin V-FITC

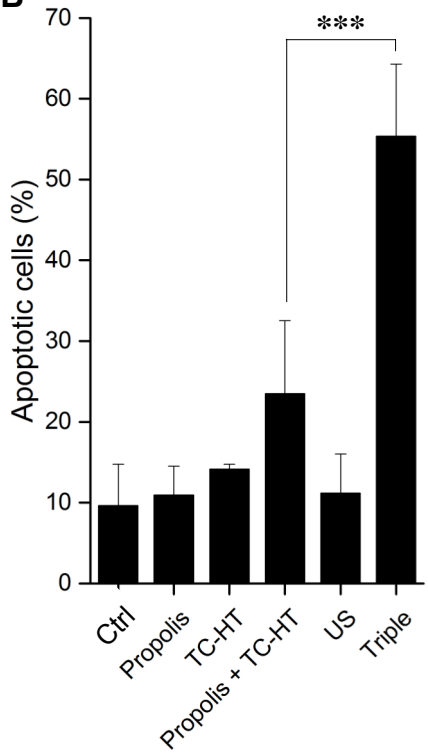
B
Apoptotic cells (%)
***
Ctrl
Propolis
TC-HT
Propolis + TC-HT
US
Triple

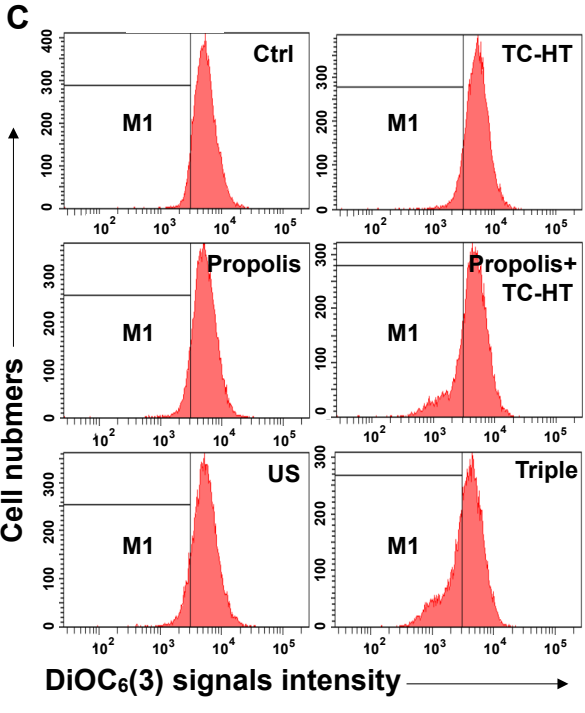
C
Ctrl
TC-HT
Propolis
Propolis+
TC-HT
US
Triple
M1
Cell nubmers
DiOC6(3) signals intensity

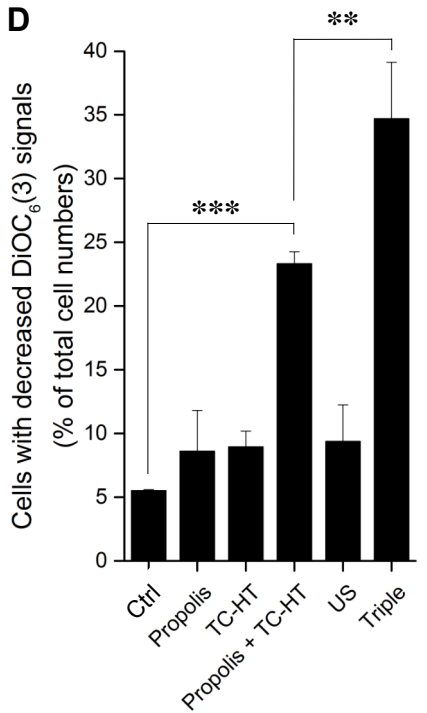
D
Cells with decreased DiOC6(3) signals
(% of total cell numbers)
**
***
Ctrl
Propolis
TC-HT
Propolis + TC-HT
US
Triple

Figure 5

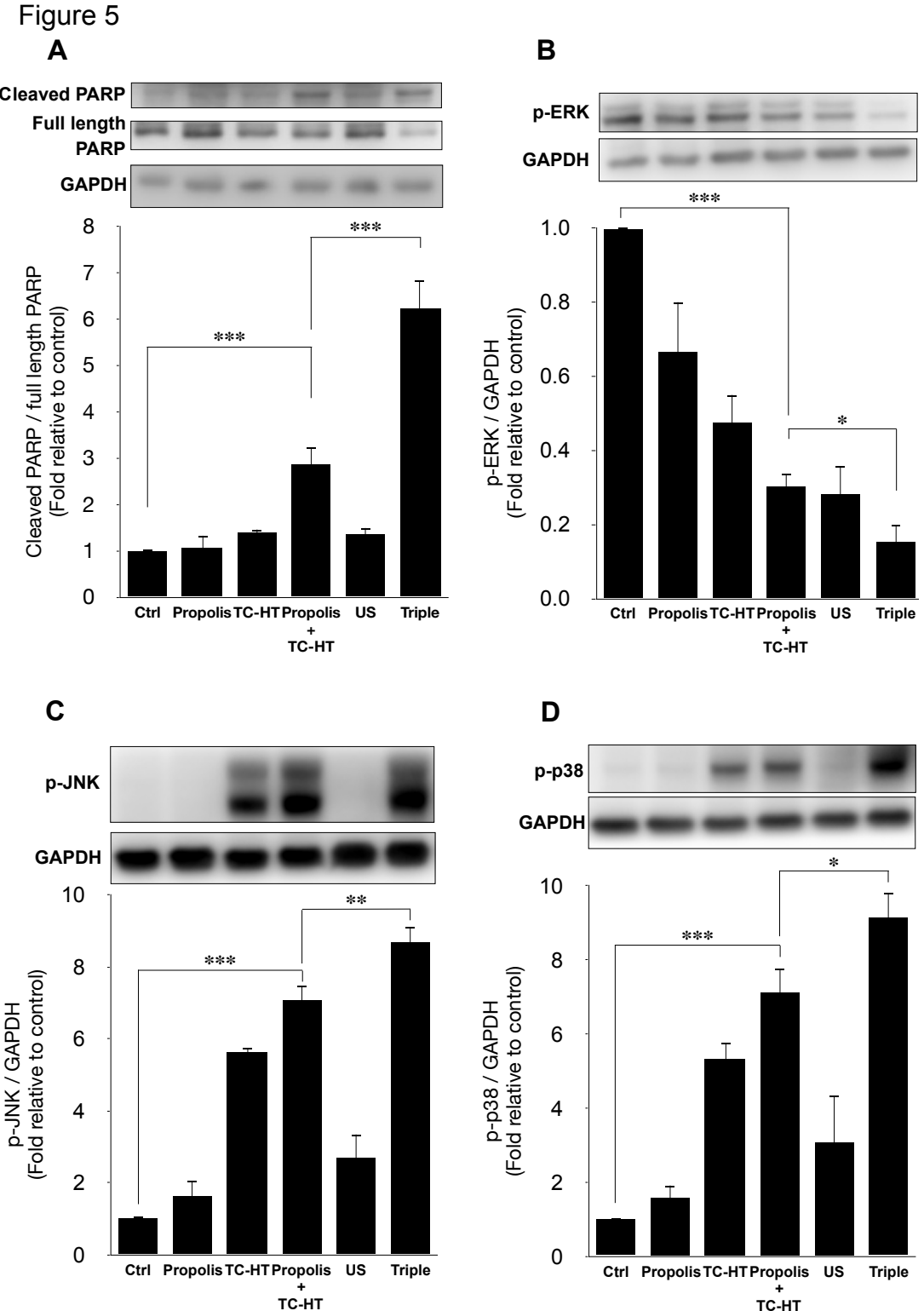
A
Cleaved PARP
Full length PARP
GAPDH
Cleaved PARP / full length PARP (Fold relative to control)
***
***
Ctrl
Propolis
TC-HT
Propolis + TC-HT
US
Triple
B
p-ERK
GAPDH
p-ERK / GAPDH (Fold relative to control)
***
*
C
p-JNK
GAPDH
p-JNK / GAPDH (Fold relative to control)
***
**
D
p-p38
GAPDH
p-p38 / GAPDH (Fold relative to control)
***
*

Figure 6

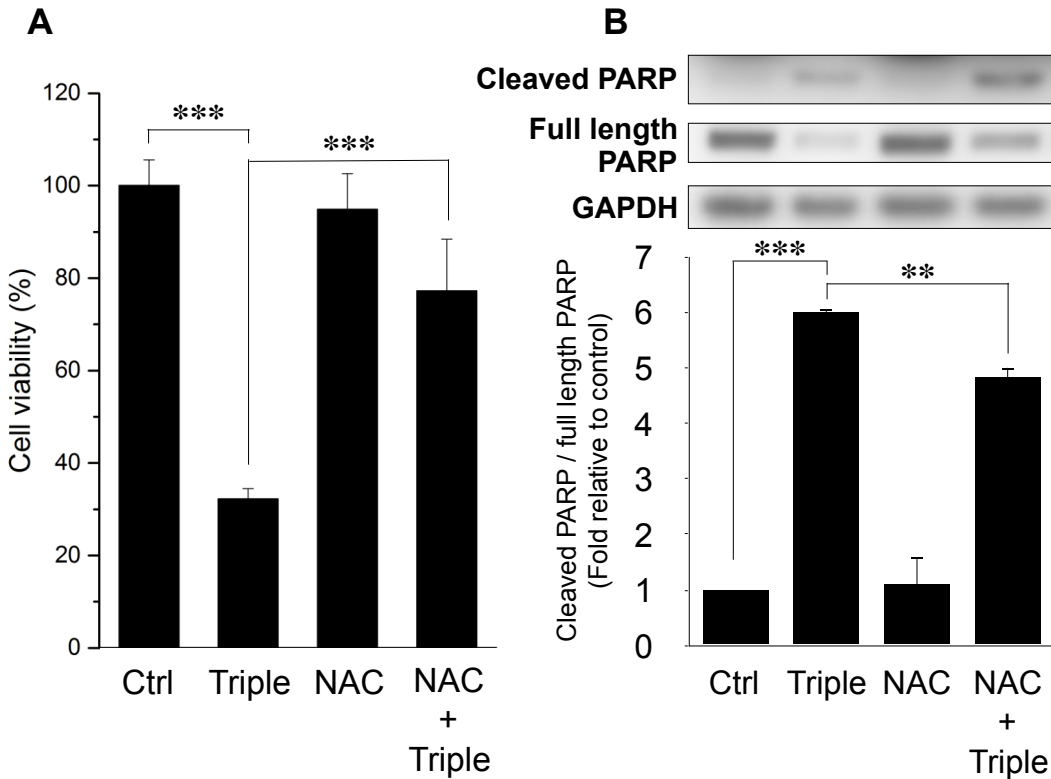
A
120
100
80
60
40
20
0
Cell viability (%)
***
***
Ctrl
Triple
NAC
NAC + Triple
B
Cleaved PARP
Full length PARP
GAPDH
7
6
5
4
3
2
1
0
Cleaved PARP / full length PARP (Fold relative to control)
***
**
Ctrl
Triple
NAC
NAC + Triple

Figure 7

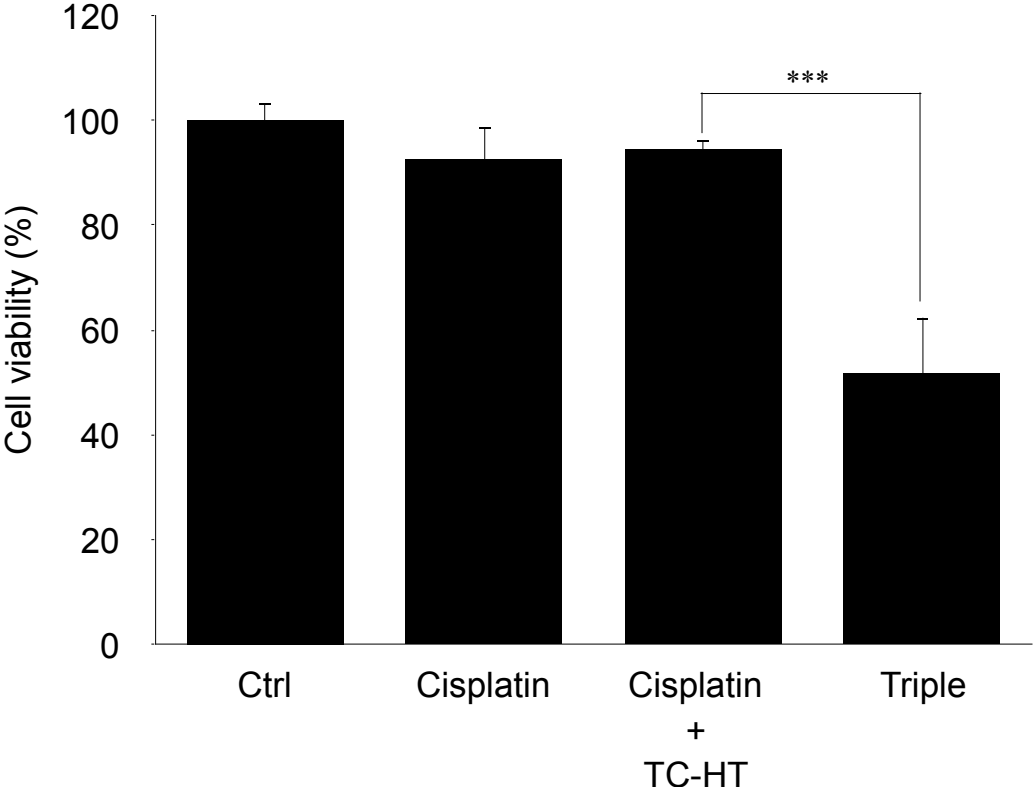
120
100
80
60
40
20
0
Cell viability (%)
***
Ctrl
Cisplatin
Cisplatin
+
TC-HT
Triple